Diagn Interv Radiol 2016; 22:291–296

NEURORADIOLOGY

ORIGINAL ARTICLE

Influence of cigarette smoking on white matter in patients with clinically isolated syndrome as detected by diffusion tensor imaging

Gamze Durhan
Sevda Diker
Arzu Ceylan Has
Jale Karakaya
Asli Tuncer Kurne
Kader Karli Oguz

PURPOSE
Cigarette smoking has been associated with increased occurrence of multiple sclerosis (MS), as well as clinical disability and disease progression in MS. We aimed to assess the effects of smoking on the white matter (WM) in patients with clinically isolated syndrome (CIS) using diffusion tensor imaging.

METHODS
Smoker patients with CIS (n=16), smoker healthy controls (n=13), nonsmoker patients with CIS (n=17) and nonsmoker healthy controls (n=14) were included. Thirteen regions-of-interest including nonenhancing T1 hypointense lesion and perilesional WM, and 11 normal-appearing white matter (NAWM) regions were drawn on color-coded fractional anisotropy (FA) maps. Lesion load was determined in terms of number and volume of WM hyperintensities.

RESULTS
A tendency towards greater lesion load was found in smoker patients. T1 hypointense lesions and perilesional WM had reduced FA and increased mean diffusivity to a similar degree in smoker and nonsmoker CIS patients. Compared with healthy smokers, smoker CIS patients had more extensive NAWM changes shown by increased mean diffusivity. There was no relationship between diffusion metrics and clinical disability scores, duration of the disease and degree of smoking exposure.

CONCLUSION
Smoker patients showed a tendency towards having greater number of WM lesions and displayed significantly more extensive NAWM abnormalities.

Clinically isolated syndrome (CIS), an inflammatory demyelinating disorder of the central nervous system, is the first clinical episode with features predictive of multiple sclerosis (MS) (1). Many environmental risk factors for conversion from CIS to MS were shown in recent studies (1, 2). Among these, cigarette smoking was shown to increase the risk of developing MS even in passive smokers (3), worsen clinical disability, and exacerbate disease progression (4) .

Diffusion tensor imaging (DTI) gives the opportunity to evaluate the tissue integrity, mainly the white matter (WM). Through changes in metrics such as fractional anisotropy (FA) and mean diffusivity (MD), DTI enables the assessment of axonal organization and myelin attenuation in addition to the WM lesions evaluated by conventional magnetic resonance imaging (MRI) sequences (5). The brains of MS patients have demonstrated that an increase in MD and a decrease in FA values were far beyond fluid attenuation inversion recovery (FLAIR) hyperintense lesions, commonly used as a clinical parameter of MS (6, 7). Brain parenchyma with no apparent lesion, namely, the normal-appearing white matter (NAWM), has drawn much attention due to the presence of not only histopathologic and radiologic abnormalities but also a close association with clinical disability and disease progression (8). Changes in the NAWM may also be responsible for the clinicoradiologic discrepancy observed in many patients (6). In addition, several MRI studies have shown significantly altered FA measures in specific brain regions in healthy smoker individuals (9, 10). Although a number of studies have investigated the impact of smoking on patients with MS (4, 11), to the best of our knowledge, no study has studied the influence of smoking on the WM in patients with CIS using DTI.

In this study we sought to determine the effects of smoking on NAWM, lesions, and perilesional WM of patients with CIS. The secondary objective was to examine whether diffu-

From the Department of Radiology (G.D.), Ministry of Health Ankara Training and Research Hospital, Ankara, Turkey; the Departments of Neurology (S.D., A.T.K.) and Radiology (K.K.O.) Hacettepe University Medical School, Ankara, Turkey; the National Magnetic Resonance Research Center (UMRAM) (A.C.H., K.K.O. ✉ *karlioguz@yahoo.com*), Bilkent University, Ankara, Turkey; the Department of Biostatistics (J.K.), Hacettepe University, Ankara, Turkey.

Received 11 September 2015;
accepted 8 October 2015.

Published online 24 March 2016.
10.5152/dir.2015.15415

sion tensor changes relate to the duration of disease, clinical disability and degree of smoking exposure.

Methods

Participants

The local institutional review board approved the study. All participants gave written informed consent.

A total of 60 right-handed subjects (33 CIS patients, 27 healthy volunteers; female (F)/male (M) ratio, 37/23; age range, 20–57 years; mean age, 31.8±8.0 years) participated in this study. Thirty-three CIS patients, admitted to our institution between 2012 and 2014 were included in the study. All patients fulfilled the McDonald diagnostic criteria for MS but had only one clinical episode involving optic neuritis, cervical and/or thoracic myelitis or brainstem/cerebellar syndrome. None of the patients converted to clinically definite MS during the study. Twenty-seven healthy volunteers were recruited using e-mail advertisement. Same individuals also constituted the participants of another MRI study on brain volume alterations. Exclusion criteria were presence of any systemic or neurologic disease other than CIS, receiving steroid therapy, having an attack within four weeks of the MRI scan, having a lifetime history of dependence disorders other than nicotine, neurologic illness other than CIS, and contraindications to MRI.

Two neurologists (S.D., A.T.) with four and 15 years of experience, blinded to the MRI findings, evaluated all patients and control subjects, and recorded expanded disability status scale scores, age at onset of smoking, pack-years of cigarettes and duration of the disease.

The subjects were categorized into four groups according to the smoking habit and presence of CIS: smoker patients with clinically isolated syndrome (CIS_S: n=16; F/M ratio, 8/8; mean age, 34.3±8.9 years), smoker healthy controls (H_S: n=13; F/M ratio, 6/7; mean age, 33.7±7.4 years), nonsmoker patients with clinically isolated syndrome (CIS_{NS}: n=17; F/M ratio, 13/4; mean age, 29.7±6.9 years), and nonsmoker healthy controls (H_{NS}: n=14; F/M ratio, 10/4; mean age, 29.8±7.9 years). Nonsmoker participants had smoked no more than five cigarettes in their lifetime.

Main points

- Clinically isolated syndrome (CIS), an inflammatory demyelinating disorder of the central nervous system (CNS), is a first clinical episode with features predictive of multiple sclerosis.
- In previous studies, cigarette smoking has been shown to increase the risk of conversion from CIS to MS, worsen clinical disability, and exacerbate disease progression.
- Compared with nonsmoker patients, smoker patients with CIS show tendency towards increased white matter lesions, in our study.
- Smoker patients with CIS exhibit more extensive normal-appearing white matter abnormalities than nonsmoker patients on diffusion tensor images.

Image acquisition

Imaging protocol included T1-weighted three-dimensional (3D) high resolution images with 0.9 mm isotropic voxels (MPRAGE) (TR/TE, 2600/3.1 ms; matrix, 224×256; NEX, 1; TA, 4.06; number of slices, 176; slice thickness, 1.00 mm; distance factor, 50%; voxel size, 1 mm; in plane resolution, 1 mm) and 3D double inversion-recovery sampling perfection with application optimized contrast using different flip angle evolution (DIR-SPACE) (TR/TE, 7500/325 ms; matrix, 192×192; NEX, 1; TA, 6.09; number of slices, 144; slice thickness, 1.12 mm without intersection gap; voxel size, 1 mm; in plane resolutions, 1 mm) imaging on 3.0 T MRI scanner (Magnetom, Tim, Siemens). This imaging sequence was selected because it enables confident lesion detection and delineation by multiplanar imaging and cerebrospinal fluid-attenuation (12, 13). Patients received intravenous gadopentetate dimeglumine (0.01 mmol/kg) contrast material. Postcontrast axial T1-weighted 3D MPRAGE coronal fat saturated images (TR/TE, 550/15 ms; matrix, 256×256; NEX, 2) were obtained at 5 min after injection in all patients to detect active demyelinating lesion.

Isotropic high-resolution diffusion tensor imaging (DTI) of the whole brain (single-shot EPI; TR/TE, 8020/83 ms; maximum b value, 1000s/mm^2; 60 independent directions; FOV, 256 mm; matrix, 128×128; 64 axial sections with 2 mm thickness without intersection gap; voxel size, 2×2×2 mm) was also selected to recognize the WM integrity.

Image processing and analysis

Immediately after image acquisition, a neuroradiologist with 14 years of experience (K.K.O.) reviewed the images to rule out any non-demyelinating lesion or to detect active demyelinating lesions. From this review, the investigator checked the radiologic eligibility of the patients for the study.

To determine lesion load in terms of number and volume, BrainVoyager QX 2.6 for Linux (http://www.brainvoyager.com) was used. Two radiologists with 5 and 14 years of experience (G.D. and K.K.O., respectively) recorded the coordination of every hyperintense WM lesion on 3D DIR SPACE imaging in consensus. The lesions were ranged by a bounding box in which all the intensities of voxels were fixed to a threshold for a clear visual distinction of lesions and parenchyma (http://support.brainvoyager.com/volume-space/107-volume-rendering/314-users-guide-masking-and-cutting.html). This was done by radiologists in consensus. In this way, the number and total volume of interests were calculated.

FSL (http://fsl.fmrib.ox.ac.uk/fsl/fslwiki/) was used for DTI data analysis. All scans were corrected for head motion, and eddy currents using the affine registration. b0 volumes of each subject were extracted and averaged. By fitting a main diffusion tensor in each voxel with FSL DTI Fit tool, the FA and MD maps were calculated. All FA, MD, pre- and postcontrast 3D T1 MPRAGE and DIR-SPACE images were registered to Montreal Neurological Institute template by FLIRT command, a part of FSL. The mean FA and MD of the regions-of-interest (ROIs), specified below were computed for each subject.

A total of 13 ROIs were manually drawn on color-coded FA maps, with a careful review of the co-registered pre- and postcontrast 3D T1-weighted images, 3D DIR-SPACE and T2 turbo spin-echo for accurate localization of ROIs of nonenhancing T1 hypointense lesion without edema in the left frontal WM (if unavailable, then right frontal WM). A perilesional WM 5 mm away from that lesion and 11 NAWM regions of 5–6 mm^2 were selected. NAWM ROIs were drawn from the genu, splenium and body of the corpus callosum, bilateral corona radiata, superior longitudinal fasciculus, posterior limb of internal capsule, and uncinate fasciculi on color-coded FA maps using Johns Hopkins University WM tractography, and the International Consortium for Brain Mapping DTI-81 WM atlases in FSL. DIR-SPACE sequence was used to avoid lesions in the determination of the NAWM ROIs (Fig. 1).

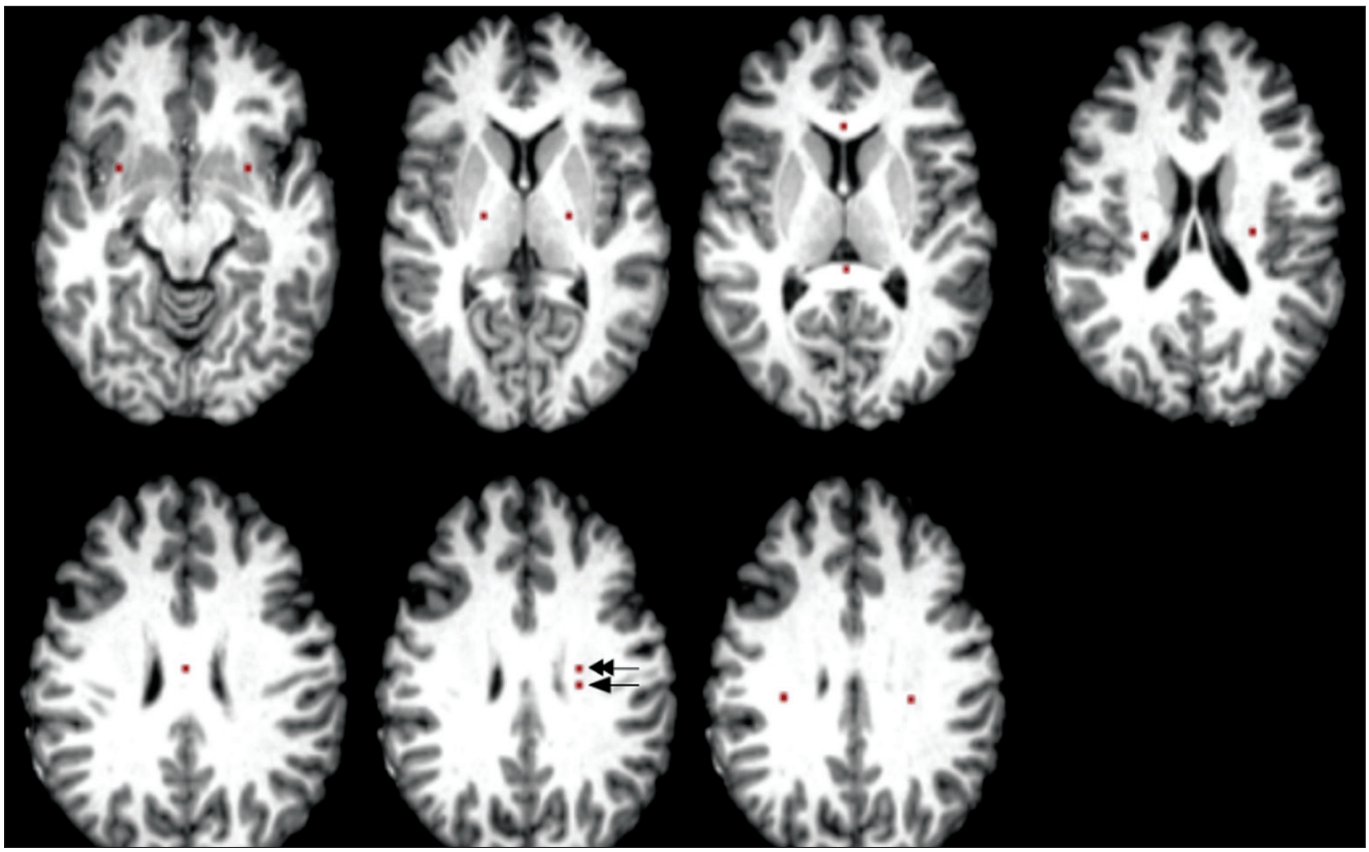

Figure 1. Placement of regions of interest (ROIs). ROIs of normal appearing white matter (NAWM) were drawn from the genu, splenium and body of the corpus callosum, bilateral corona radiata, superior longitudinal fasciculus, posterior limb of internal capsule, and uncinate fasciculi. Lesion (*arrow*) and perilesional (*double arrow*) ROIs were drawn on the left frontal white matter.

Statistical analysis

Numerical variables were evaluated for normality of data distribution using the Kolmogorov-Smirnov test. Descriptive statistics were expressed as mean±standard deviation. Independent samples t-test was performed to compare the means of two groups. The Mann Whitney U test was used to compare two groups of nonparametric data. One-way analysis of variance (One-way ANOVA) was performed to compare the differences between groups. Spearman's rho correlation coefficient was used to examine the relationship between two variables. Multiple linear regression was carried out to assess the association between two or more independent variables and a single continuous dependent variable. The analysis was also used to assess whether confounding exists. The effect of group on dependent variables was examined by multiple linear regression model, after adjustment for age and sex. A P value ≤ 0.05 was accepted as significant. Data analysis was performed by IBM SPSS Statistics 21.0 software (IBM Corp.).

Table 1. Baseline demographic characteristics, clinical data, and smoking history

	CIS_S (n=16)	CIS_{NS} (n=17)	H_S (n=13)	H_{NS} (n=14)	*P*
Age (years)	34.3±8.9	29.7±6.9	33.7±7.4	29.8±7.9	0.226
Sex (Female/male), n	8/8	13/4	6/7	10/4	0.223
Pack-year	9.3±10.1	-	7.7±4.7	-	0.904
Cigarettes per day	14.3±10.6	-	12.9±6.6	-	0.760
Duration of smoking (years)	11.6±8.5	-	12.6±8.8	-	0.680
Age at onset of smoking (years)	20.6±5.4	-	21.0±5.8	-	0.716
Time lapse from clinical episode (months)	10.8±16.5	9.2±7.0	-	-	0.313
EDSS	0.06	0.18	-	-	0.600

Data are presented as mean±SD, unless otherwise noted.

CIS_S, smoker patients with clinically isolated syndrome; CIS_{NS}, nonsmoker patients with clinically isolated syndrome; H_S, smoker healthy controls; H_{NS}, nonsmoker healthy controls; EDSS, expanded disability status scale.

Results

The demographic and clinical features of the patients are summarized in Table 1. There was no significant difference between CIS_S and H_S, nor between CIS_{NS} and H_{NS} in terms of age and sex. Furthermore, age- and sex-corrected analyses were used. Exposure to smoking, which was assessed by mean pack-years, mean cigarettes/day, age at onset of smoking and duration of smoking, was similar in CIS_S and H_S. CIS_S and CIS_{NS} showed no difference in duration of disease (10.8 vs. 9.2 months, $P > 0.05$) and expanded disability status scale (0.06 vs. 0.18, $P > 0.05$).

The review of DIR-SPACE and postcontrast 3D T1-weighted images showed no edematous and/or contrast-enhanced de-

myelinating lesions. ROIs of T1 hypointense lesions and perilesional WM could be placed over the left frontal WM in all patients.

CIS_S had a greater number and volume of WM hyperintense lesions than CIS_{NS} on DIR-SPACE imaging (15 vs. 11, $P = 0.20$ and 5.2 cm^3 vs. 2.4 cm^3, $P = 0.24$), although the difference did not reach statistical significance.

Significantly decreased FA and increased MD values were found in perilesional WM and lesions compared with those of NAWM in both CIS_S (mean values: FA=0.33, MD=0.96 for lesions; FA=0.43, MD=0.84 for perilesional WM; FA=0.62, MD=0.77 for NAWM) and CIS_{NS} (mean values: FA=0.34, MD=0.98 for lesions; FA=0.47, MD=0.83 for perilesional WM; FA=0.64, MD=0.75 for NAWM) ($P < 0.05$, for all). Compared with perilesional WM and NAWM, lesions showed significantly decreased FA and increased MD in CIS_S and CIS_{NS} ($P < 0.05$, for all). However, FA and MD measures from the lesions and perilesional WM did not differ significantly between CIS_S and CIS_{NS} ($P > 0.05$, for all) (Fig. 2).

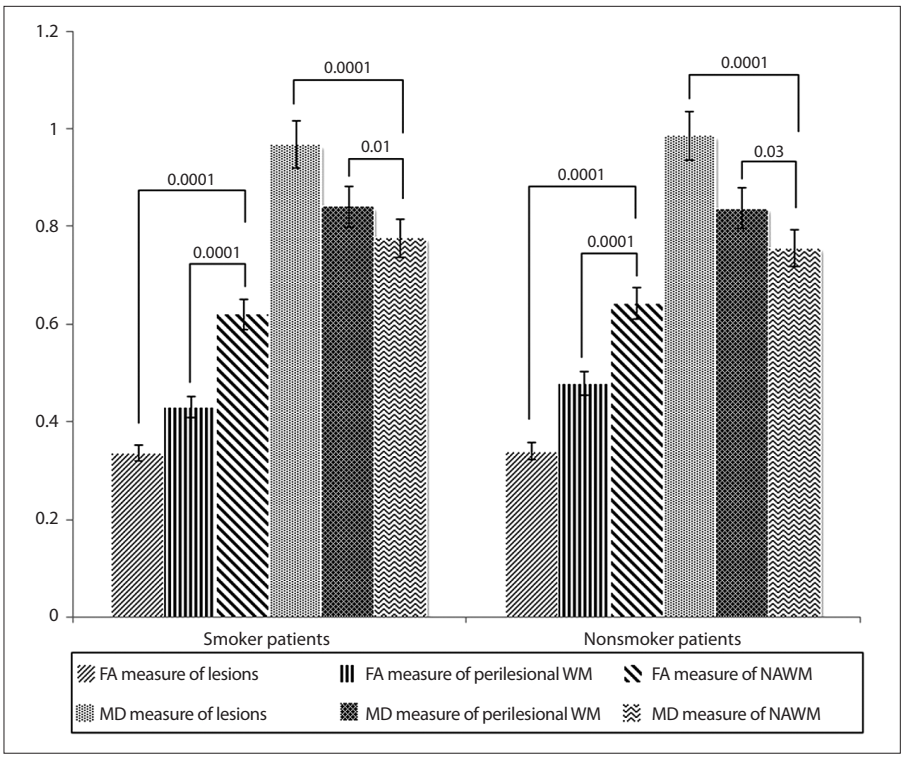

Figure 2. Comparison of mean fractional anisotrophy (FA) and mean diffusivity (MD) measurements from T1 hypointense lesions, perilesional white matter (WM) and normal appearing white matter (NAWM). Statistical significance level is given between the bars for each comparison.

Regions of NAWM with significant FA and/or MD differences in the patient and control groups are presented in Table 2. Compared with H_S, CIS_S showed elevated MD in the splenium of corpus callosum, bilateral corona radiate, and superior longitudinal fasciculus ($P < 0.05$, for all). Among the nonsmokers, a higher MD in the right corona radiata was found in CIS_{NS} than H_{NS} ($P = 0.02$). There was no brain region where CIS_S and CIS_{NS} had significantly lower MD values than their matched controls. Compared with H_{NS}, CIS_{NS} showed increased FA values in three regions of the NAWM including the body of corpus callosum, left superior longitudinal fasciculus and left posterior limb of the internal capsule ($P < 0.05$, for all). None of the NAWM regions showed significant FA change in H_S vs. CIS_S patients ($P > 0.05$, for all).

Compared with H_{NS}, H_S showed no region of FA alteration, while revealing significantly decreased MD values in the left corona radiata and superior longitudinal fasciculus ($P < 0.05$, Table 2).

In CIS patients, the mean MD value in the left superior longitudinal fasciculus was significantly higher in smokers than nonsmokers ($0.78\pm0.03\times10^{-3}$ mm^2/s vs. $0.75\pm0.04\times10^{-3} mm^2/s$, $P = 0.01$; Table 2).

Correlation analysis failed to reveal any significant relationship between DTI measures and the duration of disease, expanded disability status scale, and exposure of smoking as assessed by pack-year calculations, cigarettes/day, age at onset, and duration of smoking ($P > 0.05$).

Discussion

We aimed to investigate smoking-related WM alterations using DTI in patients with CIS in comparison with healthy controls matched for smoking habit. We calculated FA and MD as the most commonly used DTI measures in chronic T1 hypointense lesions, perilesional WM, and NAWM far from the lesions (14). On *ex vivo* MRI, chronic, nonenhancing T1 hypointense lesions, so called "black holes," show hypocellularity, reduced axonal density, decreased myelin and greater matrix disruption compared with non-black hole lesions histopathologically (15). These lesions usually show the greatest WM injury, as also supported by findings of magnetic resonance spectroscopy and magnetization transfer imaging (16). In agreement with previously published reports (5, 17), we found the most significant changes in FA and MD values in T1 hypointense lesions, followed by perilesional WM and NAWM of the patients compared with NAWM of the healthy controls. FA, generally regarded as a measure of WM integrity, is closely related with axonal caliber and the surrounding myelin. MD gives a measure of the average molecular motion depending on cellular size, compartmental fluid imbalance, and degradation products (14, 18). With the abovementioned histopathologic abnormalities in myelin and accompanying primary or secondary axonal loss, reduced FA and elevated MD were expected changes in the WM of our patients with demyelinating disease.

Our study revealed a trend for a greater lesion load on double inversion recovery sequence in smoking patients, although it was not statistically significant. Furthermore, smoker patients had evidently more extensive NAWM changes than nonsmokers (in five ROIs vs. one ROI) compared with matched healthy controls. Additional deteriorating effects of the toxic contents of tobacco smoke such as cyanide, nitric oxide, and free radicals might explain the greater vulnerability of the NAWM in CIS_S. The associations between thiocyanate, the main metabolite of cyanide and demyelination in the central nervous system of animals (19), and between nitric oxide and axonal degeneration, blocks in axonal conduction, especially in demyelinated axons (20) are well known. Through increased axonal de-

Table 2. FA and MD readings in normal-appearing white matter regions across the groups

	FA readings			
NAWM regions	CIS_S/H_S	CIS_{NS}/H_{NS}	H_S/H_{NS}	CIS_S/CIS_{NS}
CC genu	0.84/0.84	0.86/0.85	0.84/0.85	0.84/0.86
CC body	0.68/0.68	0.71/0.65[a]	0.68/0.65	0.68/0.71
CC splenium	0.87/0.88	0.87/0.86	0.88/0.86	0.87/0.87
R corona radiata	0.46/0.49	0.49/0.53	0.49/0.53	0.46/0.49
L corona radiata	0.49/0.53	0.51/0.53	0.53/0.53	0.49/0.51
R SLF	0.56/0.59	0.54/0.56	0.59/0.56	0.56/0.54
L SLF	0.54/0.58	0.59/0.55[b]	0.58/0.55	0.54/0.59
R uncinate fasciculus	0.51/0.58	0.51/0.53	0.58/0.53	0.51/0.51
L uncinate fasciculus	0.45/0.49	0.52/0.52	0.49/0.52	0.45/0.52
R PLIC	0.69/0.62	0.68/0.65	0.62/0.65	0.69/0.68
L PLIC	0.68/0.62	0.73/0.65[b]	0.62/0.65	0.68/0.73
	MD readings			
	CIS_S/H_S	CIS_{NS}/H_{NS}	H_S/H_{NS}	CIS_S/CIS_{NS}
CC genu	0.74/0.62	0.70/0.68	0.62/0.68	0.74/0.70
CC body	0.82/0.74	0.80/0.78	0.74/0.78	0.82/0.80
CC splenium	0.75/0.65[a]	0.76/0.68	0.65/0.68	0.75/0.76
R corona radiata	0.77/0.69[b]	0.74/0.71c	0.69/0.71	0.77/0.74
L corona radiata	0.77/0.68[b]	0.75/0.74	0.68/0.74c	0.77/0.75
R SLF	0.77/0.72[d]	0.77/0.75	0.72/0.75	0.77/0.77
L SLF	0.78/0.69[a]	0.75/0.74	0.69/0.74[b]	0.78/0.75[a]
R uncinate fasciculus	0.78/0.73	0.80/0.77	0.73/0.77	0.78/0.80
L uncinate fasciculus	0.80/0.74	0.77/0.75	0.74/0.75	0.80/0.77
R PLIC	0.74/0.69	0.73/0.73	0.69/0.73	0.74/0.73
L PLIC	0.76/0.69	0.71/0.73	0.69/0.73	0.76/0.71

Data represent mean FA and MD ($\times 10^{-3}$ mm^2) measurements in four matched groups.
FA, fractional anisotropy; MD, mean diffusivity; NAWM, normal-appearing white matter; CIS_S, smoker patients with clinically isolated syndrome; H_S, smoker healthy controls; CIS_{NS}, nonsmoker patients with clinically isolated syndrome; H_{NS}, nonsmoker healthy controls; CC, corpus callosum; R, right; L, left; SLF, superior longitudinal fasciculus; PLIC, posterior limb of the internal capsule.
[a]$P = 0.01$; [b]$P = 0.03$; [c]$P = 0.02$; [d]$P = 0.002$.

generation, smoking has been blamed for a worse clinical course in MS (21).

With no apparent change in FA, decreased MD in the left corona radiata and superior longitudinal fasciculus of H_S may be due to nicotine-related alterations in the WM. The nicotine-induced cytotoxic swelling suggested by Gazdzinski et al. (22) and proinflammatory effects of cigarette smoke on tissue as shown by elevated peripheral leukocytes, and recruitment of polymorphonuclear cells, monocytes, macrophages, and increased fibrinogen may be partly responsible for cellular edema and reduced MD levels in the H_S of the current study (23). Some recent studies have hypothesized on the neurotropic and promyelinating effects of smoking and have found higher FA in brain regions such as the prefrontal WM, cingulum, and corpus callosum in smokers compared with nonsmokers (9, 24). Yet, another study on heavy smokers reported decreased FA in the anterior corpus callosum (25). The variable degrees of addiction of smoking in the participants might be one important factor in these contradictory research findings. Although limited dependence and exposure to nicotine revealed no significant change, heavy smoking exposure showed marked FA reductions in WM (9, 24). Whether FA or MD is more sensitive and an earlier measure of WM disintegrity remains controversial in the literature (26, 27).

We failed to show a significant correlation of DTI measures with exposure of smoking or duration of the disease in our relatively homogeneous patient group of CIS. This might have resulted from limited cigarette smoking exposure and relatively short duration of disease as well as the younger age of our patients.

Interestingly, CIS_{NS} in comparison with H_{NS} revealed increased FA in several regions of the NAWM. Increased intracellular water resulting in cellular swelling, fiber reorganization or remyelination can account for an increase in FA (14, 28). Similar findings have been previously shown in the NAWM of patients with chronic recurrent inflammatory optic neuropathy, in T1-hyperintense lesions and normal appearing tissue in patients with MS. The authors attributed these findings to remyelination and glial activation (29, 30). Low expanded disability status scale and absence of conversion to MS during the two years of the study may have been partly related to remyelination in the NAWM, occurring as a compensatory mechanism. More heterogeneous histopathologic processes rather than uniform demyelination or axonal degeneration may be present in the NAWM of patients with CIS.

The limitations of the current study warrant discussion. First, the number of subjects was relatively small. Second, we could not avoid gender disproportion in the smoking and nonsmoking groups because women usually show less tendency to smoke in our population. To minimalize this limitation we used age- and sex-corrected analysis. Finally, it was not possible to compare the conversion rate of CIS to MS in smokers vs. nonsmokers due to the relatively short time period of the study. Therefore, studies with more individuals, more detailed characterization of smoking behavior and a longer follow-up are needed.

In conclusion, CIS and smoking appear to cause variable changes on the WM. Smoking patients showed a tendency towards greater numbers of demyelinating WM lesions and significantly more extensive NAWM abnormalities on DTI. Our findings support the adverse effects of smoking on the WM, which in turn may be related with the clinical course of CIS and conversion to MS.

Acknowledgements

The authors thank the National Magnetic Resonance Imaging Research Centre (UMRAM) for providing the MRI facility and

Yıldıray Gökhalk for his help in data acquisition.

Conflict of interest disclosure

The authors declared no conflicts of interest.

References

1. Miller DH, Chard DT, Ciccarelli O. Clinically isolated syndromes. Lancet Neurol 2012; 11:157–169. [CrossRef]
2. Mandia D, Ferraro OE, Nosari G, Montomoli C, Zardini E, Bergamaschi R. Environmental factors and multiple sclerosis severity: a descriptive study. Int J Environ Res Public Health 2014; 11:6417–6432. [CrossRef]
3. Hedstrom AK, Baarnhielm M, Olsson T, Alfredsson L. Exposure to environmental tobacco smoke is associated with increased risk for multiple sclerosis. Mult Scler 2011; 17:788–793. [CrossRef]
4. Di Pauli F, Reindl M, Ehling R, et al. Smoking is a risk factor for early conversion to clinically definite multiple sclerosis. Mult Scler 2008; 14:1026–1030. [CrossRef]
5. Filippi M, Cercignani M, Inglese M, Horsfield MA, Comi G. Diffusion tensor magnetic resonance imaging in multiple sclerosis. Neurology 2001; 56:304–311. [CrossRef]
6. Ciccarelli O, Werring DJ, Wheeler-Kingshott CA, et al. Investigation of MS normal-appearing brain using diffusion tensor MRI with clinical correlations. Neurology 2001; 56:926–933. [CrossRef]
7. Yu CS, Lin FC, Liu Y, Duan Y, Lei H, Li KC. Histogram analysis of diffusion measures in clinically isolated syndromes and relapsing-remitting multiple sclerosis. Eur J Radiol 2008; 68:328–334. [CrossRef]
8. Filippi M, Comi, G., Rovaris, M. Normal-appearing white and grey matter damage in multiple sclerosis. 1st ed. Milano: Springer, 2004; 3–8.
9. Paul RH, Grieve SM, Niaura R, et al. Chronic cigarette smoking and the microstructural integrity of white matter in healthy adults: a diffusion tensor imaging study. Nicotine Tob Res 2008; 10:137–147. [CrossRef]
10. Gons RA, van Norden AG, de Laat KF, et al. Cigarette smoking is associated with reduced microstructural integrity of cerebral white matter. Brain 2011; 134:2116–2124. [CrossRef]
11. Salzer J, Hallmans G, Nystrom M, Stenlund H, Wadell G, Sundstrom P. Smoking as a risk factor for multiple sclerosis. Mult Scler 2013; 19:1022–1027. [CrossRef]
12. Kober T, Granziera C, Ribes D, et al. MP2RAGE multiple sclerosis magnetic resonance imaging at 3 T. Invest Radiol 2012; 47:346–352. [CrossRef]
13. Wattjes MP, Lutterbey GG, Gieseke J, et al. Double inversion recovery brain imaging at 3T: diagnostic value in the detection of multiple sclerosis lesions. AJNR Am J Neuroradiol 2007; 28:54–59.
14. Beaulieu C. The basis of anisotropic water diffusion in the nervous system - a technical review. NMR Biomed 2002; 15:435–455. [CrossRef]
15. van Walderveen MA, Kamphorst W, Scheltens P, et al. Histopathologic correlate of hypointense lesions on T1-weighted spin-echo MRI in multiple sclerosis. Neurology 1998; 50:1282–1288. [CrossRef]
16. van Walderveen MA, Barkhof F, Pouwels PJ, van Schijndel RA, Polman CH, Castelijns JA. Neuronal damage in T1-hypointense multiple sclerosis lesions demonstrated in vivo using proton magnetic resonance spectroscopy. Ann Neurol 1999; 46:79–87. [CrossRef]
17. Oguz KK, Kurne A, Aksu AO, Taskiran A, Karabulut E, Karabudak R. A comparative assessment of cerebral white matter by magnetization transfer imaging in early- and adult-onset multiple sclerosis patients matched for disease duration. J Neurol 2010; 257:1309–1315. [CrossRef]
18. Pierpaoli C, Jezzard P, Basser PJ, Barnett A, Di Chiro G. Diffusion tensor MR imaging of the human brain. Radiology 1996; 201:637–648. [CrossRef]
19. Van Houten WH, Friede RL. Histochemical studies of experimental demyelination produced with cyanide. Exp Neurol 1961; 4:402–412. [CrossRef]
20. Redford EJ, Kapoor R, Smith KJ. Nitric oxide donors reversibly block axonal conduction: demyelinated axons are especially susceptible. Brain 1997; 120:2149–2157. [CrossRef]
21. Sundstrom P, Nystrom L. Smoking worsens the prognosis in multiple sclerosis. Mult Scler 2008; 14:1031–1035. [CrossRef]
22. Gazdzinski S, Durazzo TC, Studholme C, Song E, Banys P, Meyerhoff DJ. Quantitative brain MRI in alcohol dependence: preliminary evidence for effects of concurrent chronic cigarette smoking on regional brain volumes. Alcohol Clin Exp Res 2005; 29:1484–1495. [CrossRef]
23. Shirani A, Tremlett H. The effect of smoking on the symptoms and progression of multiple sclerosis: a review. J Inflamm Res 2010; 3:115–126. [CrossRef]
24. Hudkins M, O'Neill J, Tobias MC, Bartzokis G, London ED. Cigarette smoking and white matter microstructure. Psychopharmacology 2012; 221:285–295. [CrossRef]
25. Lin F, Wu G, Zhu L, Lei H. Heavy smokers show abnormal microstructural integrity in the anterior corpus callosum: a diffusion tensor imaging study with tract-based spatial statistics. Drug Alcohol Depend 2013; 129:82–87. [CrossRef]
26. Werring DJ, Clark CA, Barker GJ, Thompson AJ, Miller DH. Diffusion tensor imaging of lesions and normal-appearing white matter in multiple sclerosis. Neurology 1999; 52:1626–1632. [CrossRef]
27. Cubon VA, Putukian M, Boyer C, Dettwiler A. A diffusion tensor imaging study on the white matter skeleton in individuals with sports-related concussion. J Neurotrauma 2011; 28:189–201. [CrossRef]
28. Le Bihan D. Looking into the functional architecture of the brain with diffusion MRI. Nat Rev Neurosci 2003; 4:469–480. [CrossRef]
29. Colpak AI, Kurne AT, Oguz KK, Has AC, Dolgun A, Kansu T. White matter involvement beyond the optic nerves in CRION as assessed by diffusion tensor imaging. Int J Neurosci 2015; 125:10–17. [CrossRef]
30. Calabrese M, Rinaldi F, Seppi D, et al. Cortical diffusion-tensor imaging abnormalities in multiple sclerosis: a 3-year longitudinal study. Radiology 2011; 261:891–898. [CrossRef]